EMPIRICAL RESPONSE SPECTRAL ATTENUATIONS ON THE ROCKS WITH VS =0.5 TO 3.0KM/S IN JAPAN

Hiroshi KAWANO[1], Katsuya TAKAHASHI[2], Masayuki TAKEMURA[3], Masanobu TOHDO[4], Takahide WATANABE[5] And Shizuo NODA[6]

SUMMARY

We evaluated an attenuation relation for response spectra of horizontal and vertical strong motions on rocks. The relation was based on waveforms observed at 12 observation stations in Japan with known underground structure from geophysical loggings etc.. For aseismic design, near-source regions are important, so we used an attenuation formula with an equivalent hypo-central distance. We evaluated the amplification factor of surface layers from the base rock as a function of S-wave or P-wave velocities. We tested the attenuation relation on strong-motion data recorded in California, Chile, Mexico, and Japan, and obtained good agreement, including data from near-source regions.

INTRODUCTION

Previous reports [1), 2)] applied the attenuation relation of response spectra for hard stratum with an equivalent hypo-central distance, to include the influence of the spread of fault planes, to near-source regions.
Near-source data are crucial to aseismic design. At the same time, by explaining the characteristics of seismic wave propagation from the base rock by earthquake observation data, collected by seismometers set in vertical array at observation stations with known underground structures, the attenuation relation is applicable to both horizontal and vertical motion. The amplification characteristics of such seismic waves in the surface layers depend on the underground structures at the observation stations; for instance, the horizontal motions depend on the velocity, Vs, of S waves, and vertical motions on the velocity, Vp, of P waves.
Putting the above relation into a model, we propose a prediction method for the strong motion spectra on rock and compare it to earthquake data in Japan and the Americas. This equation, moreover, uses earthquake motion on base rock and in-ground amplification factor during its travel to the rock surface in a pair.

DATA

We used the observation stations and epicenters of earthquakes shown in Figure 1; this totaled 107 records (simultaneous recording of two directions of horizontal components with vertical component) of 44 earthquakes. The magnitudes M, depths of hypocenters, H, and hypo-central distances, X, of the earthquakes were $5.5 \leqq M \leqq 7.0$, $0 \leqq H \leqq 60$ km and $27 \leqq X \leqq 20$ 2 km, respectively. Used were data either recorded at ground surfaces where $0.5 \leqq Vs \leqq 2.7$ km/s ($1.7 \leqq Vp \leqq 5.5$ km/s), or obtained by analytically removing the effects of the uppermost surface layers of the ground from underground observation data (or by stripping-off analysis) using the

underground structure [3), 4)]. Their maximum acceleration ranged from 1 to 210 gals and averaged about 20 gals. The stripping-off analysis was done with a soil structure model. The latter was made by optimizing the mean amplification characteristics of the ground at each observation station. The Kodamagawa observation station

[1] *Nuclear Power Engineering Dept.,Tokyo Electric Power Company Email: T0742742@pmail.tepco.co.jp*
[2] *Kajima Technical Research Institute,Kajima Corporation Email: katsuta@katri.kajima.co.jp*
[3] *Kobori Research Complex,Kajima Corporation Email: takemura@krc.kajima.co.jp*
[4] *Institute of Construction Technology,Toda Corporation Email: masanobu.todo@toda.co.jp*
[5] *Ohsaki Research Institute Email: wtaka@ori.shimz.co.jp*
[6] *Nuclear Power Engineering Dept.,Tokyo Electric Power Compan Email: T0542761@pmail.tepco.co.jp*

(KDG) had ground equivalent to seismic bedrock, Vs = 2.2 km/s. Here we used a waveform obtained by modifying a higher-than-5-Hz spectrum into a semi-infinite ground equivalent, and included the influence of topography [5), 6)]. Analysis was limited to both horizontal and vertical motions coming after the arrival of the first S wave because frequently these cause ground motions crucial to aseismic design [7)]. Moreover, data from observation stations where seismometers were arrayed to the depth of seismic bedrock showed that even when the surface layers of the ground were generally controlled by S waves, their vertical motion was influenced to a greater extent by P waves converted from S waves near seismic bedrock [7), 8)]. The analysis of vertical motion in this study is from these results.

ANALYSIS

Attenuation method

We used the following equation, with known physical parameters, to estimate attenuation.

$$\log Si(T) = a(T)M-\{b(T)Xeq+\log Xeq\}+ci(T) \quad (1)$$

where Si (T) is the acceleration response spectrum (damping constant 5%), i indicates observation station; and a (T), b (T), and ci (T) are regression coefficients, of which relations with the physical parameters were known [9)], and Xeq[10)] is the equivalent hypo-central distance. The latter can represent the spread of fault planes, and was used to evaluate seismic motions near their source (see Equation (7)).

Spectra on seismic bedrock

Figure 2 shows regression coefficients a, b, and c0 in solid lines. They were determined with data at locations equivalent to seismic bedrock from horizontal motion in equation (1). Coefficients a and b, in broken lines, were from vertical motion data and the same equation. The two different sets of a and b agree with each other. This agreement suggests that vertical and horizontal components were caused by seismic S waves that changed after arriving at seismic bedrock. This is because a and b represent the spectrum characteristics of incident waves[9)] that are influenced only by the source and propagation. We found that the Q value of the propagation route, evaluated in terms of coefficient b, was about $120f^{0.85}$ in the frequency range of 0.5 to 20 Hz, in agreement with other studies. As earlier papers [1), 2)] suggest, Midorikawa and Kobayashi's spectra of incident waves on seismic bedrock [11)] was a little larger than that from the ground layer equivalent to seismic bedrock, the latter determined by the horizontal motion regression formula.

Amplification in the surface layer

When the amplification factor for horizontal motion was determined from the ratio of the horizontal spectrum at each observation station to the horizontal motion spectrum on the ground layer equivalent to seismic bedrock from data recorded at KDG, the logarithm of the amplification factor, di (T) was

$$di(T) = ci(T) - c0(T) \quad (2)$$

where c0 (T) is the regression coefficient for the data observed at the ground layer equivalent to seismic bedrock. A regression calculation by equation (1) was done by substituting coefficients a and b from horizontal motion for those from vertical motion since the former nearly equaled the latter. As a result, the logarithm of the amplification factor, dvi (T), the ratio of vertical motion at each observation station to the horizontal motion on the ground layer equivalent to seismic bedrock, is given by

$$dvi(T) = cvi(T) - c0(T) \quad (3)$$

where cvi (T) is the regression coefficient for vertical motion at each observation station, and c0 (T) is the regression coefficient for horizontal motion data on the ground layer equivalent to seismic bedrock. Because the influence of the incident angle on the ratio of the vertical to horizontal spectrum on the seismic bedrock is minor, it was ignored.

Equations (2) and (3) determine in-ground amplification factors for a range of horizontal and vertical motion periods for the spectrum on seismic bedrock, respectively. Figure 3 shows the relation between the in-ground amplification factors, and Vs at the observation station (black circles). White circles denote earthquake motions on the ground at the Tomioka observation station (TMK) [12)]. They were determined analytically by assuming the upper part of surface layer to be exposed at various depths in a vertical array of seismometers. The two sets of

circles agree well with each other and indicate that the dependency of the amplification factors on Vs increases with the period. This agrees with a previous study [5]. The solid line in the figure is

$$10^{d(f)} \propto (1/Vs)^{\delta h(T)} \quad (4)$$

In a very short period range of 0.02 to 0.05 seconds, $\delta h(T) = 0.0$, which increase with the period; in the period range of 2.0 to 5.0 seconds, $\delta h(T) = 0.83$. Thus, the amplification factor was negligible at small periods, but gradually increased with the period to about 1.4 at a Vs of 1.5 km/s, and to about 2.6 at a Vs of 0.7 km/s at long periods. Similarly, the in-ground amplification of vertical motion depended on Vp, and was about 1.4 at a Vp of 3 km/s, and about 2.3 when Vp equaled 2 km/s.

FOMULARIZATION

We calculated the mean response spectrum of earthquake motion from the above results. We will limit this to periods between 0.02 and 5 seconds, and on rocks within 200 km of the hypo-central distance. With these restrictions, Vs was between about 0.5 and 3 km/s for earthquakes of magnitude greater than 5.5 with hypo-central depth less than 60 km.

The mean response spectrum of horizontal earthquake motion

The mean acceleration response spectrum of horizontal earthquake motion on the rock surface, Sh (T) (cm/s^2), was calculated by Equation (5) with a 5% damping factor. The mean response spectrum on seismic bedrock, Sb(T), was multiplied by the in-ground amplification correction term [$\alpha h(T) \cdot \beta h(T)$]. The former depended on the velocity Vs (km/s) of S waves at the rock surface. The latter depended on the primary predominant period Ts1(s) of the surface layer, i.e., the region between the seismic bedrock and the rock surface. The $\beta h(T)$ was put in the equation because the earthquake motion was independent of in-ground amplification at periods greater than the primary predominant period of the surface layer[13].

$$Sh(T) = Sb(T)\,\alpha h(T)\,\beta h(T) \quad (5)$$

while

$$\log Sb(T) = a(T)M - \{b(T)Xeq + \log Xeq\} + c0(T) \quad (6)$$

where M is the Japan Meteorological Agency magnitude, Xeq is the equivalent hypo-central distance (km) given by

$$Xeq^{-2} = \int em\,Xm^{-2}\,ds \,/ \int em\,ds \quad (7)$$

where Xm is the distance (km) between the observation station and each small area on the plane of the earthquake-generating fault, em is the distribution of energy released from each small area on the fault plane and set to one when unknown, $\int ds$ is the integration on the fault plane; and a (T), b (T), and c0 (T) are the regression coefficients shown in Figure 2.
The in-ground amplification factor, $\alpha h(T)$, which depended on the velocity of S waves at the surface layer, and the coefficient $\beta h(T)$, which makes the in-ground amplification correction term equal to one at periods sufficiently greater than the primary predominant period of the surface layer, are given by the following equations.

$$\begin{aligned} \alpha h(T) &= (Vs/Vsb)^{-\delta h(T)} && (T \leqq Ts1) \\ &= (Vs/Vsb)^{-\delta h(Ts1)} && (T > Ts1) \end{aligned} \quad (8)$$

$$\begin{aligned} \beta h(T) &= 1 && (T \leqq Ts1) \\ &= (T/Ts1)^{-\log(\alpha h(Ts1))} && (10Ts > T > Ts1) \\ &= 10^{-\log(\alpha h(Ts1))} && (T \geqq 10Ts1) \end{aligned} \quad (9)$$

Vsb, the velocity of S waves in seismic bedrock, equaled 2.2 km/s. Table 1 presents $\delta h(T)$; Figures 4 and 5 show examples of $\alpha h(T)$, and $\beta h(T)$ calculations, respectively.

The mean response spectrum of vertical earthquake motion

The mean acceleration response spectrum of vertical earthquake motion on the rock surface, Sv (T) (cm/s^2), was calculated by Equation (10) with a 5% damping factor. The mean response spectrum on seismic bedrock in Equation (2), Sb (T), was multiplied by the in-ground amplification correction term [αv (T) · βv (T)]. The former depended on the velocity Vp (km/s) of P waves at the rock surface. The latter depended on the primary predominant period Tp1 (s) of the surface layer.

$$Sv(T) = Sb(T)\,\alpha v(T)\,\beta v(T) \tag{10}$$

The in-ground amplification factor αv (T) depended on the P wave velocity at the surface layer and the coefficient βv (T), which makes the in-ground amplification correction term equal to αbv (Tp1) at periods sufficiently greater than the primary predominant period of the surface layer, are given by the following equations.

$$\begin{aligned} \alpha v(T) &= \alpha bv(T)\,(Vp/Vpb)^{-\delta v(T)} && (T \leqq Tp1) \\ &= \alpha bv(Tp1)\,(Vp/Vpb)^{-\delta v(Tp1)} && (T > Tp1) \end{aligned} \tag{11}$$

$$\begin{aligned} \beta v(T) &= 1 && (T \leqq Tp1) \\ &= (T/Tp1)^{-\log\{\alpha v(Tp1)/\alpha bv(Tp1)\}} && (10Tp1 > T > Tp1) \\ &= 10^{-\log\{\alpha v(Tp1)/\alpha bv(Tp1)\}} && (T \geqq 10Tp1) \end{aligned} \tag{12}$$

Vpb, the velocity of P waves in the seismic bedrock, equaled 4.2 km/s. αbv (T) is the ratio of vertical to horizontal motion at the seismic bedrock, which comes from Equation (3) when cvi (T) is replaced with the vertical motion observed on the ground layer equivalent to seismic bedrock. Table1 presents δv (T) and αbv (T); and Figures 6 and 7 show examples of calculated αv (T), and βv (T), respectively. We calculated the vertical to horizontal response spectrum ratio on the ground layer equivalent to seismic bedrock (where Vs = 2.2 km/s and Vp = 4.2 km/s), and the same ratio for the rock surface (where Vs = 0.7 km/s and Vp = 2.0 km/s) from Equations (5) and (10). They were both approximately 0.6 (see Figure 8).

EXAMINATION OF APPLICABILITY

Comparison of the trial prediction with overseas records

The prediction method was evaluated by comparison to overseas observation data from near-source regions. Compared were 14 records from 7 earthquakes at 10 observation stations with known underground structures and Vs$\geqq$0.5 km/s. They were in California, Mexico, and Chile. Table 2 shows the list of overseas records used for checking applicability. In this comparison, 5.7$\leqq$M$\leqq$8.1 and 14.0$\leqq$Xeq$\leqq$76.9 km. The Xeq values[14] that had the locations, forms, slip distributions, and other fault plane data were used because those records included that taken from near-source regions. The shortest distance along the ground to the faults from the observation stations, Xsh, were between 4.1 and 52.2 km. The velocities here were 0.76$\leqq$Vs$\leqq$2.2 km/s and 0.85$\leqq$Vp$\leqq$3.9 km/s. All of the observation stations specialized in measurements on the ground surface. Being unavailable, the primary predominant periods of the surface layers, Ts1 and Tp1, were set to five seconds. This corresponded to the case where there was no reduction in in-ground amplification for periods greater than the primary predominant period.

Figure9 shows the vertical ratios of the estimated to observed spectra in a stack, the mean of the logarithms of the ratios, and the mean ± standard deviation. This result indicates good agreement between the two sets of spectra. The dispersion in the figure, which is almost equal to that when the regression formula was applied to the original data. Previous papers[15] reported the same result on the horizontal motion. One reason for this could be that, detailed data on overseas fault planes were inputted in the equivalent hypo-central distance calculation. Specifically, both the horizontal and vertical motion observed in the Coyote Lake earthquake at Girrloy #1 of which shortest distance was about 11 km from the fault agreed very well with the trial prediction, as Figure10 illustrates.

When the above ratios were about one, the prediction method produced satisfactory mean values. Similar comparisons made between trial predictions by the formula and other domestic records had nearly the same results.

Cases of Near-Fault Rupture Directivity Effect

A phenomenon recently attracting attention is the predominance of long-period pulses in the fault-normal component in the direction of rupture propagation[16]. This phenomenon, the near-fault rupture directivity effect

or NFRDE, is when the amplitude of seismic waves increases in the fault-normal component because of its radiation pattern and directivity due to the source mechanism. This rupture propagation effect occurs in near-source regions where there are fewer disturbances in the seismic wave propagation routes. On the other hand, while capable of including the influence of fault plane spreading by applying the equivalent hypo-central distance to the attenuation equation, the prediction method applies to short-period earthquake motion and does not include both the source mechanism and the rupture propagation effect above. The latter are parameters with less influence on earthquake motion prediction. Therefore, when the influence of those parameters dominates, as in the NFRDE, the prediction method is probably less valid.

Figure 11 compares the observation data, recorded at Kobe University, on the Hyogoken-Nanbu earthquake, which had a powerful NFRDE, with our trial prediction of the same earthquake. The prediction method nearly reproduced both the observed vertical and horizontal components, although it generally overestimated the horizontal components and underestimated the NS components of periods greater than one second that crossed the fault rupture line almost at right angles. Including the increment by NFRDE from the study of Ohno et al.[17] is considered to make the prediction method applicable even to near-source regions with a dominant NFRDE.

CONCLUSION

Using seismic waveforms from 12 earthquake observation stations with known underground structures, we evaluated a method to predict the horizontal and vertical motion response spectra on rock surface. An attenuation equation with an equivalent hypo-central distance was introduced so that the prediction method could be applied to near-source regions, where data is crucial for aseismic design. Moreover, the prediction method could evaluate the amplification characteristics of seismic waves in the surface layer with increased accuracy by using S and P wave velocities as parameters. The comparison of observed strong motion waveforms to prediction indicated that the method was accurate near-source regions.

ACKNOWLEDGMENTS

This study is jointly founded by ten electric power companies in Japan. We thank Emeritus Professors Shunitiro Omote of Kyushu Sangyo University and Hiroyoshi Kobayashi of Tokyo Institute of Technology for valuable comments and advice given during this study. We also thank Professor Tokiharu Ohta at Ashikaga Institute of Technology for assistance promoting this study for more than 15 years since it began.

REFERENCES

1. Takahashi,K.,M.Takemura,O.Chiba,T.Watanabe,Y.Shikama:Attenuation Curves on Pre-Quaternary Grounds Part1 Horizontal Component, Summaries of Technical Papers of Annual Meeting AIJ,363-364,1994 (in Japanese)
2. Tohdo,M.,T.Hatori,K.Takahashi,T.Watanabe,Y.Shikama:ditto Part2 Vertical Component,Summaries of Technical Papers of Annual Meeting AIJ,365-366,1994 (in Japanese)
3. Takemura,M.,T.Ikeura,K.Takahashi,H.Ishida,Y.Ohshima:Attenuation Characteristics of Seisimic Waves in Sedimentery Layers and Strong Motion Estimation,Journal of Struct. Constr.Eng,AIJ,No.446,1-11,1993 (in Japanese with English abstract)
4. Tohdo,M.,T.Hatori,O.Chiba,K.Takahashi,M.Takemura,H.Tanaka:Characteristics of Vertical Seisimic Motions and Qp-Values in Sedimentery Layers,,Journal of Struct. Constr.Eng,AIJ,No.475,45-54,1995 (in Japanese with English abstract)
5. Takemura,M., K. Kato, T. Ikeura, and E. Shima, : Site amplification ofS-waves from strong motion records in special relatin to surface geology,J. Phys. Earth, 39,537-552,1991
6. Kato,K.,M.Takemura , T. Ikeura,K.Urao,and T.Uetake:Preliminary analysis for evaluation of local site effects from strong motion spectra by an inversion method,J. Phys. Earth,40 175-191,1992
7. Takahashi,K.,S.Ohno,M.Takemura,T.Ohta,T.Hatori,Y.Sugawara,T.Hatori and S.Omote:Observation of earthquake strong-motion with deep borehole-Generation of vertical motion propagating in surface layers after S-wave arrival-,Proc.Tenth World Conf.Earthq.Eng.,Vol.3, 1245-1250,1992
8. Uetake,T.,Y.Sugawara,Y.Ohshi,K.Takahashi,T.Hatori,M.Tohdo,O.Chiba,R.Hukuzawa:A study on characteristics of vertical earthquake motions in array observations Part1:Amplifications of vertical earthquake ground motions on observation records,Summaries of Technical Papers of Annual Meeting AIJ,,305-306,1990 (in Japanese)
9. Takemura,M.,T.Ohta,S.Hiehata:Theoretical Basis of Empirical Relations about Response Spectra of Strong Ground-Motions,Journal of Struct. Constr.Eng,AIJ,No.375, 1-9,1987 (in Japanese with English abstract)
10. Ohno,S., T. Ohta, T. Ikeura, and M. Takemura, : Revision of attenuation formula considering the effect of

fault size to evaluate strong motionspectra in near field, Tectonophysics,218, 69-81, 1993
11. Midorikawa,S.,H.Kobayashi:Spectral Characteristics of Incident Wave from Seismic Bedrock due to Earthquake,Journal of Struct. Constr.Eng,AIJ,No.273,43-54,1978 (in Japanese with English abstract)
12. Ikeura,T.,S.Omote,T.Yamashita,T.Ohta,K.Takahashi,H.Ishida:A Sudy on Characteristics of Seismic Motions in the Rock with Vertical Instrument Array Part15:Removal of Local Characteristics of Surface Geology from observed Seismic Motion Records,Summaries of Technical Papers of Annual Meeting AIJ,751-752,1989 (in Japanese)
13. Kobayashi,H.,S.Nagahashi:Amprification Characteristics of the Ground and Spectral Characteristics of Earthquake Motions on the Seismic Bedrock inferred from Spectral Characteristics of Earthquake Motions observed on the Ground Surface,Journal of Struct. Constr.Eng,AIJ,No.240, 79-92,1976 (in Japanese with English abstract)
14. Ohno,S.,M.Takemura,M.Niwa,and K.Takahashi:Intensity of strong ground motion on Pre-Quaternary stratum and surface soil amprifications durring the 1995 Hyogo-ken Nanbu Earthquake,Japan,J. Phys. Earth,44,623-648, 1996
15. Takahashi,K.,M.Takemura,M.Tohdo, T.Watanabe and S.Noda: Empirical response spectral attenuations on the rocks with Vs =0.5 to 3.0 km/s, in Japan,The 10th Japan Earthq.Eng.Sym.,1998.11 (in Japanese with English abstract)
16. Somerville,P.,N.Smith,N.Abrahamson:Representation of Near-Fault RuptureDirectivity Effect in Design Ground Motions,and Apprication to CaltransBridges,National Seismic Conference on Bridges and Highways,1995
17. Ohno,S.,M.Takemura,Y.Kobayashi:Near-Fault Rupture Directivity Effects on Strong-Motion Records,The 10th Japan Earthq.Eng.Sym.,133-138,1998 (in Japanese with English abstract)

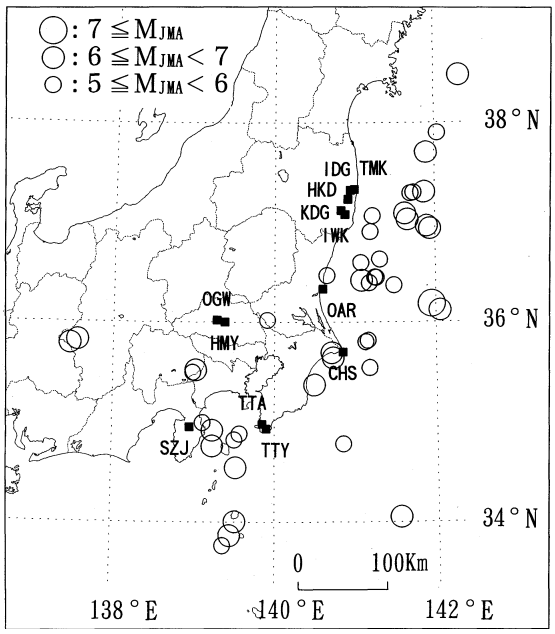

Figure 1 Distribution of epicenters and magnitudes recorded for 107 records and location of

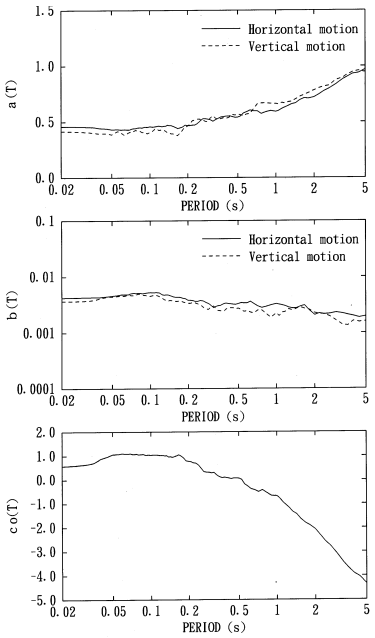

Figure 2 Estimated regression coefficients

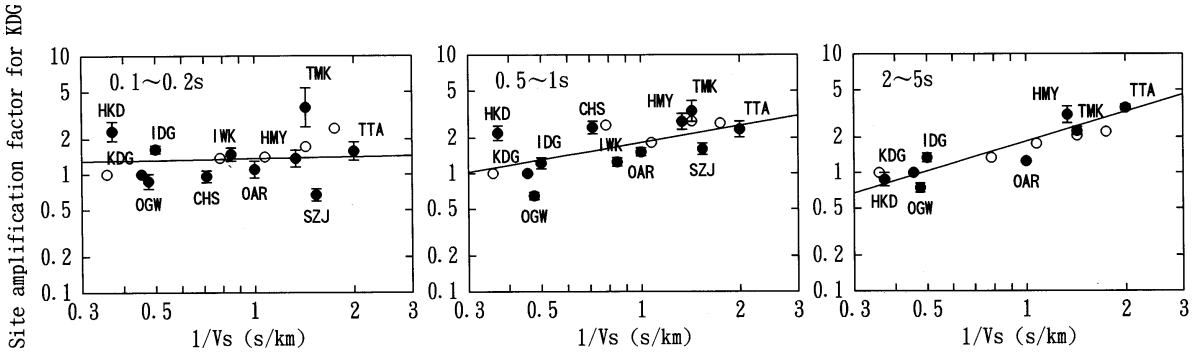

Figure 3 Relation between site amplification factor and S-wave velocity of surface layer

Table 1 List of site amplification factors δh, δv and ratio of vertical to horizontal

Period (s)	0.02~0.05	0.05~0.1	0.1~0.2	0.2~0.5	0.5~1.0	1.0~2.0	2.0~5.0
Center Period (s)	0.03	0.07	0.14	0.32	0.71	1.40	3.20
δh(T)	0.00	0.01	0.05	0.37	0.48	0.71	0.83
δv(T)	0.12	0.14	0.47	0.69	0.95	1.12	1.09
αbv(T)	0.58	0.58	0.51	0.60	0.55	0.66	0.75

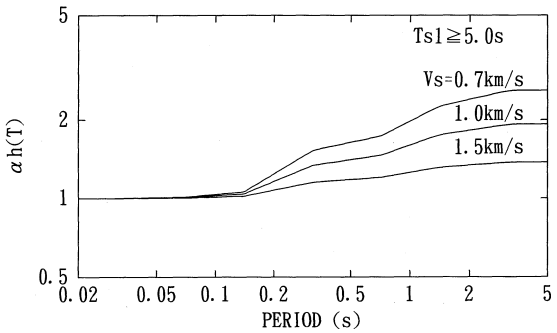

Figure 4 Coefficient of site amplification factor αh as a function of S-wave velocity

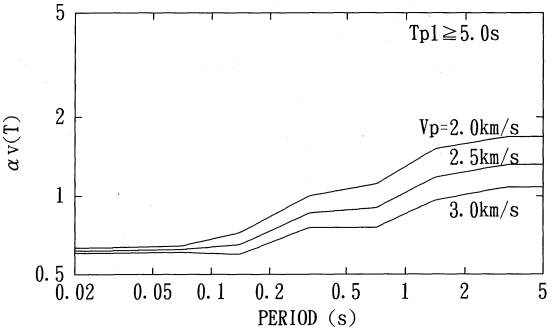

Figure 6 Coefficient of site amplification factor αv as a function of P-wave velocity

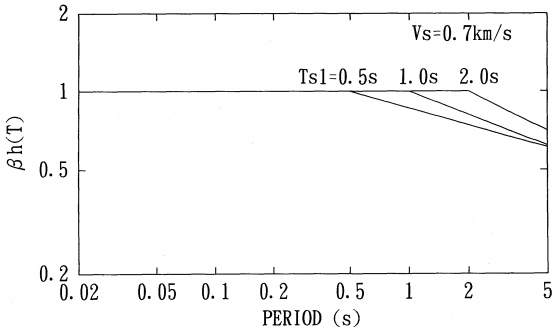

Figure 5 Relation between long period reduction coefficient βh and 1st predominant period of surface layer

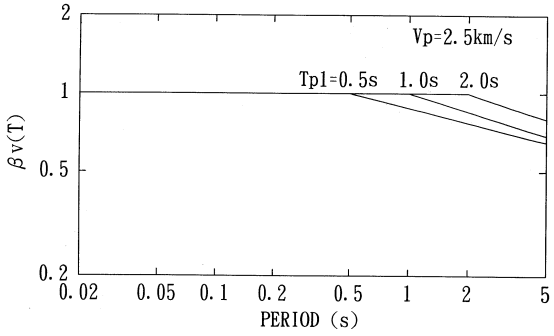

Figure 7 Relation between long period reduction coefficient βv and 1st predominant period of surface layer